GPS-assisted GLONASS orbit determination

D. Kuang, Y. E. Bar-Sever, W. I. Bertiger, K. J. Hurst, J. F. Zumberge

Jet Propulsion Laboratory, California Institute of Technology, Pasadena, CA 91109, USA
e-mail: da.kuang@jpl.nasa.gov; Tel.: +1-818 354-8332; Fax: +1-818-393-4965

Abstract. Using 1 week of data from a network of GPS/GLONASS dual-tracking receivers, 15-cm accurate GLONASS orbit determination is demonstrated with an approach that combines GPS and GLONASS data. GPS data are used to define the reference frame, synchronize receiver clocks and determine troposphere delay for the GLONASS tracking network. GLONASS tracking data are then processed separately, with the GPS-defined parameters held fixed, to determine the GLONASS orbit. The quality of the GLONASS orbit determination is currently limited by the size and distribution of the tracking network, and by the unavailability of a sufficiently refined solar pressure model. Temporal variations in the differential clock bias of the dual-tracking receivers are found to have secondary impact on the orbit determination accuracy.

Key words: GPS – GLONASS – Orbit

1 Introduction

The International GLONASS Experiment 1998 (IGEX-98) (Slater et al. 1998) provided the first organized global GLONASS tracking data for the study of GLONASS orbit modeling and orbit determination.

  GLONASS satellites orbit the Earth at an altitude comparable to that of the GPS satellites, and transmit similar radio ranging and navigation signals. Our approach to GLONASS orbit determination draws from techniques developed at the Jet Propulsion Laboratory (JPL) to determine the orbit of other Earth orbiters that transmit GPS-like signals (Wu 1985; Haines et al. 1995). We use the GIPSY-OASIS II software package (Wu et al. 1990) to analyze a week of GLONASS and GPS

tracking data (GPS Week 996), and conduct several experiments with the GLONASS orbit determination.

2 A method for GLONASS orbit determination

Some of the receivers that track GLONASS signals can also track GPS signals simultaneously. The common information carried in both GPS and GLONASS tracking data at these stations includes station position, receiver clock bias, and tropospheric delay. This allows us to tie both GPS and GLONASS orbits to the same reference system. GPS is a more mature system. First, the GPS data is much stronger than the GLONASS data due to better geometry and shear quantity, as there are twice as many functioning GPS satellites as there are GLONASS satellites. Second, the GPS dynamic and measurement models are much better understood than those of GLONASS. Daily GPS orbit solutions accurate to 10 cm and transmitter clock bias solution good to 0.2 ns are available from International GPS Service for Geodynamics analysis centers (see e.g. Jefferson et al. 1999). The precise point positioning technique (Zumberge et al. 1997) allows us to use previously determined GPS orbit and clock solutions to estimate site position, receiver clock bias, and tropospheric delay solutions for any given site. These products and techniques allow us to use the GPS tracking data to define a precise reference frame for the GLONASS tracking network, synchronize receiver clocks and determine the troposphere delay for the stations occupied by dual-tracking receivers.

  Our data processing is performed in a two-step procedure. First, we use the precise point positioning technique with GPS orbits and clock determined from the large IGS network to estimate all the station-specific parameters. These parameters tie the GLONASS tracking network to the reference system defined by the precise GPS orbit and clock. In the second step, we process the GLONASS tracking data from all receivers (including those that only tracked GLONASS and not GPS), with the parameters solved from the first step held fixed, to determine the orbit of GLONASS satellites.

Correspondence to: D. Kuang

This procedure provides us with convenience and flexibility to conduct various experiments, in the second step only, to study GLONASS-specific issues.

In each of the two steps described above, we process undifferenced ionosphere-free pseudorange and phase measurements. The station-specific parameters solved in the first step are: the constant station position, the receiver clock bias as a white-noise process, and the zenith tropospheric delay as a random-walk process. The GPS orbit and transmitter clock parameters are fixed to the precise ephemerides and clock corrections produced by the IGS/FLINN (Fiducial Laboratorial International Natural-Science Network) process at JPL (Jefferson et al. 1999). The solutions in this step tie the dual-tracking stations to the reference frame in which the GPS ephemerides are defined (ITRF96 in this case). We refer to these stations as *fiducial* for GLONASS orbit determination. We refer to the stations that track GLONASS satellites only as *non-fiducial* stations. In the second step we determine the precise orbits and transmitter clock biases of the GLONASS satellites. This second step also determines the non-fiducial (GLONASS-only receivers) station positions, receiver clock biases, and tropospheric delays. At each fiducial site we estimate a differential clock bias between the GPS tracking and GLONASS tracking in the second step.

The differential clock bias between GPS tracking and GLONASS tracking is a feature of the GPS/GLONASS dual-tracking receivers. Because the GPS and the GLONASS signals are at different frequencies, they incur different latencies as they are processed in the receiver's electronics. This causes the apparent bias between the GPS-based receiver clock estimate and the GLONASS-based receiver clock estimate. This differential clock bias may be manufacturer-dependent, receiver-dependent, and/or time-dependent. One of the advantages of our approach is the flexibility in modeling this differential clock bias. In our process, GPS-based receiver clock estimates at the fiducial sites are synchronized to the GPS system clock through precise point positioning to tenths of a nanosecond. The differential clock bias between GPS tracking and GLONASS tracking for dual-tracking receivers can be modeled as either a constant or a stochastic process.

According to the Russian Space Agency (Revnivykh and Mitrikas 1998), the attitude control scheme of GLONASS satellites is similar to that of GPS satellites, with the navigation antenna pointing to the geocenter, and with yaw attitude and solar array pitch for optimal solar power. Thus, we use the GPS Block II solar radiation pressure to model the GLONASS solar radiation pressure. In addition to the six epoch-state parameters, we estimate for each GLONASS satellite a constant solar scale and Y-Bias, and stochastic accelerations in the satellite body-fixed system to compensate for un-modeled perturbations. Alternatively, empirical periodical force models can be used to approximate the mis-modeled non-gravitational forces.

Since GLONASS tracking data are sparser than GPS, we process longer, 3-day arcs, unlike the typical 30-hour arcs used for GPS processing. The middle 30-hour orbit of each of the moving 3-day orbit arc is taken as the solution orbit, and 6-hour orbit overlap difference with neighboring orbit arcs is evaluated to assess the orbit precision.

3 Experiments

We chose to process dual-frequency measurement only to remove the ionosphere delay effects. Three types of dual-frequency receivers were used during Week 996 in IGEX-98: Ashtech Z18, 3S Navigation R100, and JPS Legacy GGD. The 3S R100 receivers track GLONASS only. There are only two JPS Legacy GGD receivers in the data set of that week; one of them did not function properly in tracking GPS satellites, and the other had only a limited amount of data in that week. As a result, all the fiducial station data come from Ashtech Z18 receivers during that week. The distribution of the tracking stations for the week is shown in Fig. 1.

In order to study the effects of the solar radiation pressure force modeling, the temporal variation of differential clock bias for dual-tracking receivers, and the stability of the reference frame, we examined the following experimental cases.

Case 1. Use GPS Block II satellite solar radiation pressure force model, and estimate stochastic accelerations along the satellite body-fixed axes. These acceleration parameters are updated every hour, with process noise sigma of 10^{-11} m/s^2, and correlation time of 4 hours. Model the differential clock biases for dual-tracking receivers as random-walk process. Fix the position of fiducial sites to the daily GPS precise point positioning solution.

Case 2. Use empirical functions to model the solar radiation pressure force, estimate constant and once-per-revolution accelerations along the directions of U (satellite-sun), V (solar-panel axis), and W (perpendicular to U and V). Other models are the same as those in case 1.

Case 3. Model the differential clock bias for dual-tracking receivers as a constant for each orbit arc (3 days). Other models are the same as those in case 1.

Case 4. Use the same strategy and models as in case 1, except that the position of fiducial sites is fixed to a combined solution over three months' precise point positioning with the GPS data from IGEX-98 (Kuang et al. 1999).

The features of these cases are summarized in Table 1. In all these cases, the differential clock bias is relative to a selected reference station, at which the differential clock bias between GPS and GLONASS tracking is fixed to zero. Case 1 is the baseline case. By comparing the results from the other three cases with that of case 1, we expect to learn about the effect of different solar radiation pressure force modeling, differential clock modeling, and the effect of reference frame stability in our approach to GLONASS orbit determination.

In all the above cases, the measurements are edited with the elevation angle cut off at 15 degrees. In our
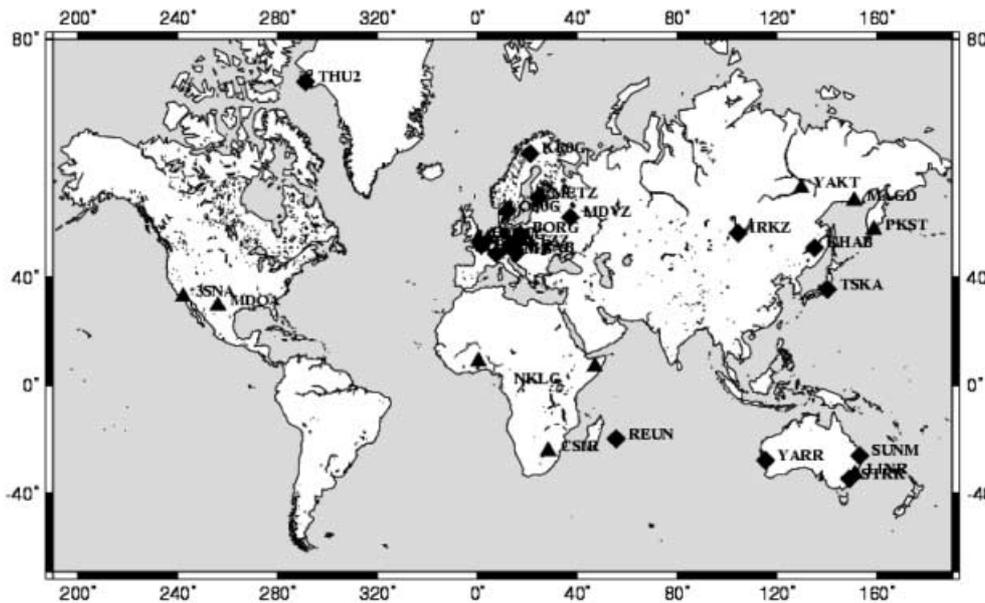
Fig. 1. Distribution of IGEX98 tracking stations during GPS Week 996. *Diamond* fiducial station; *triangle* non-fiducial station

Table 1. Experimental cases

Case	Differential clock bias	Solar radiation pressure	Position of fiducial sites
Case 1	Random walk	Stochastic	Daily solution
Case 2	Random walk	Once per revolution	Daily solution
Case 3	Constant	Stochastic	Daily solution
Case 4	Random walk	Stochastic	Combined solution

Table 2. Additional experimental cases

Case	Differential clock bias	Readjust troposphere delay	Elevation angle cut off (degrees)
Case 5	Constant	Random walk	15
Case 6	Random walk	Fixed	7
Case 7	Constant	Fixed	7

process the GLONASS tracking data does not contribute to the determination of troposphere delay, even though the line of sight to GLONASS satellites may differ from those to GPS satellites at the same station. In order to study the potential effects of tropospheric delay errors, we designed the following additional experimental cases.

Case 5. Estimate the zenith troposphere delay, on top of the GPS solution, as a random-walk process. Other models are same as those in case 3.

Case 6. Edit the measurement with elevation angle cut-off at 7 degrees. Other models are same as those in case 1.

Case 7. Edit the measurement with elevation angle cut-off at 7 degrees. Other models are same as those in case 3.

The features of these additional cases are summarized in Table 2. Lowering the elevation cut-off angle in cases 6 and 7 increases the amount of GLONASS tracking data by about 10% as compared to the corresponding cases 1 and 3. The number of total data points processed on each day is shown in Table 3.

Table 3. Number of data points processed on each day

Date	With 15-degree elevation cut off	With 7-degree elevation cut off	Increase of data amount (%)
02/07/2000	81 116	84 069	3.6
02/08/2000	79 004	84 745	7.2
02/09/2000	98 467	104 693	6.3
02/10/2000	87 262	96 406	10.5
02/11/2000	90 985	100 722	10.7
02/12/2000	91 552	102 408	11.8
02/13/2000	96 658	108 179	11.9

4 Results and summary

In order to compare the GLONASS orbit solutions from the different experimental cases, we use the median overlap difference as a measure of the orbit accuracy. That is, for each satellite we take the median of the RMS orbit overlap differences over the six overlapping sessions in the week as the measure of the orbit accuracy. While imperfect, past experience with satellites for which independent verification of orbit accuracy is available (such as GPS and TOPEX/Poseidon) has suggested that orbit overlap is a fairly robust measure for orbit accuracy (Bertiger et al. 1994). Another measure for the performance of orbit models is the RMS of data fit residual. The results are presented in Figs. 2 through 7.

4.1 Data strength

Compared to the abundance of GPS tracking data that are regularly processed in general GPS orbit determination practice, there are far less GLONASS tracking data
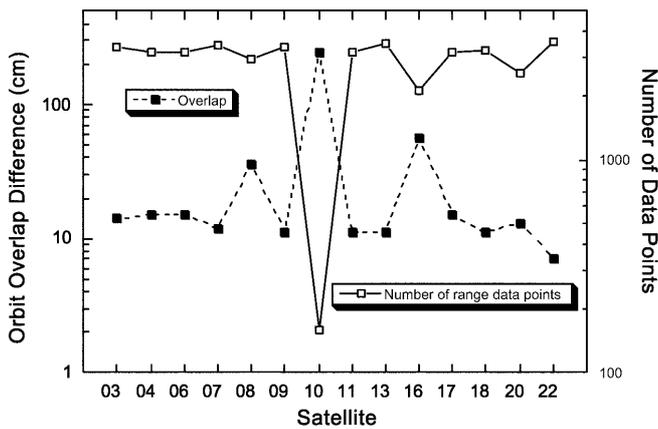
Fig. 2. Median orbit overlap difference and number of data points

from IGEX-98. Although we use three days' data to determine one orbit arc, some satellites are still not well determined due to data weakness. Figure 2 shows the median of 3-D orbit overlap differences from case 3, and the average number of range data points involved in one orbit arc solution for each satellite. It clearly demonstrates the correspondence between the orbit quality and the data strength. The orbits of satellites 10 and 16 are significantly less accurate than those of other satellites because of the relatively smaller amount of valid data. With such weak data it is not possible to solve for a large number of parameters for better dynamic and measurement modeling.

All seven experimental cases result in similar data fit for pseudorange measurements. Carrier phase data residual RMS values are slightly different for each case, as shown in Fig. 3. It is not surprising that cases 6 and 7 have the highest residual RMS among the seven cases, because there are more low-elevation data in these cases. Cases 2 and 3 have the medium residual level, higher than that of cases 1 and 4, because fewer parameters are estimated in the former two cases. However, these two cases result in quite different orbit overlaps, revealing the differences in the dynamic modeling.
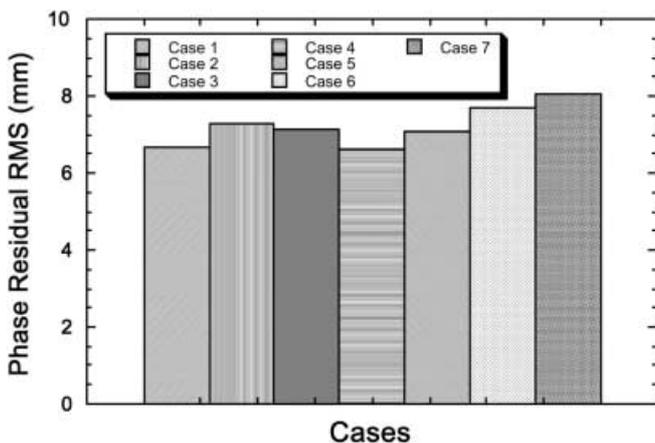
4.2 Solar radiation pressure models

Figure 4 shows the orbit overlap differences for cases 1 through 4. Case 2 has noticeably higher orbit overlap difference than the other three cases. This demonstrates that the solar radiation pressure force modeling is an important factor in the GLONASS orbit determination. The relatively long orbit arc (3-day arc compared to 1-day GPS orbit arc in IGS processes) requires better dynamics modeling. Since we use the solar radiation pressure model for GPS Block II satellites as the nominal model for GLONASS satellites, the actual force may not be modeled well due to the different structure (e.g. a GLONASS satellite has a cylinder bus) and material of the GLONASS satellites. During GPS Week 996, all the 12 functioning GLONASS satellites are in full sun. During shadow period, the difference between the two systems would be even more complicated. Estimating stochastic accelerations to compensate for the different dynamics works reasonably well, as indicated by the orbit overlap difference of cases 1, 3, and 4. Theoretically, this approach should work for any satellite as long as there is sufficient data strength to resolve the perturbation time series. However, the approach of updating stochastic accelerations becomes invalid when the data strength is weak. A refined solar radiation pressure model with a smaller number of parameters to adjust is needed in such cases. The result of case 2 indicates that a simple once-per-revolution force model cannot do the job. A model devoted particularly to GLONASS spacecraft, either an empirical model derived from tracking data (Ineichen et al. 1999), or an analytical model (Ziebart 1999) similar to ROCK4 (Fliegel et al. 1992), will help the situation.

4.3 Reference frame stability

Cases 1 and 4 give very similar orbit overlap differences, as shown in Fig. 4. They also result in almost the same data fit residual RMS, as shown in Fig. 3. This illustrates the high quality of our daily GPS precise
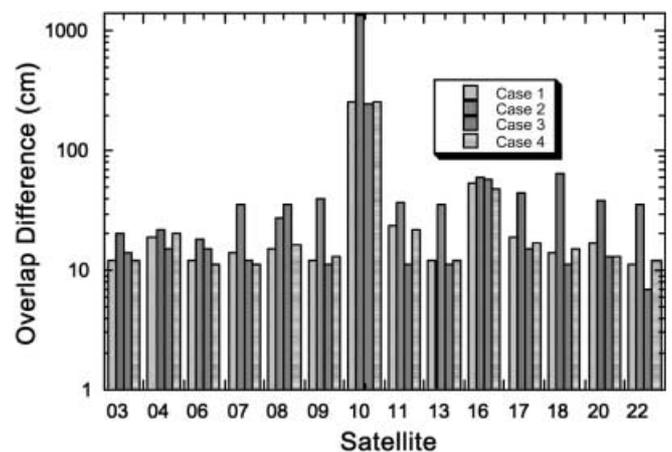

Fig. 3. Weekly average carrier phase data residual RMS for each case

Fig. 4. Median orbit overlap difference for cases 1 through 4

point positioning solution, as the effect of day-to-day variations of the fiducial site position solutions seems negligible at the current orbit precision level.

4.4 Differential clock biases

The comparison between cases 1 and 3 shows that the effect of temporal variations in the differential clock bias on the orbit is also very small. Modeling the differential clock bias as constant may actually result in slightly better orbit overlaps, as shown in Fig. 4. Figure 5 shows the differential clock biases estimated as constant from case 3, during the 4 days in the week that station KHAB is taken as the reference station for the differential clock bias. The estimated values of these differential clock biases do change from day to day at the 10-cm level. The random-walk model in case 1 also recovers consistent drift of the differential clock biases in different orbit arc solutions, as shown in Fig. 6. However, the effect of these temporal variations on the orbit solution is reduced by the averaging over the tracking network and over time. With the constant model the recovered bias is essentially an average of the random-walk process, as shown in Fig. 6. Most of the unmodeled effects manifest as data residuals, thus the RMS of the data fit residual in case 3 is noticeably higher than that of cases 1 and 4.

4.5 Troposphere delay representative error

In case 5 we readjust the zenith troposphere delay as a random-walk process instead of letting the differential clock bias vary temporally. The data fit residual RMS in case 5 is almost the same as that in case 3, but noticeably higher than that of cases 1 and 4, as shown in Fig. 3. The orbit overlap differences in case 5 also remain about the same as in case 3 (Fig. 7). This is further evidence for the existence of temporal variation in the differential clock biases, because readjusting the zenith delay cannot take the signal out of the residual. This also confirms the
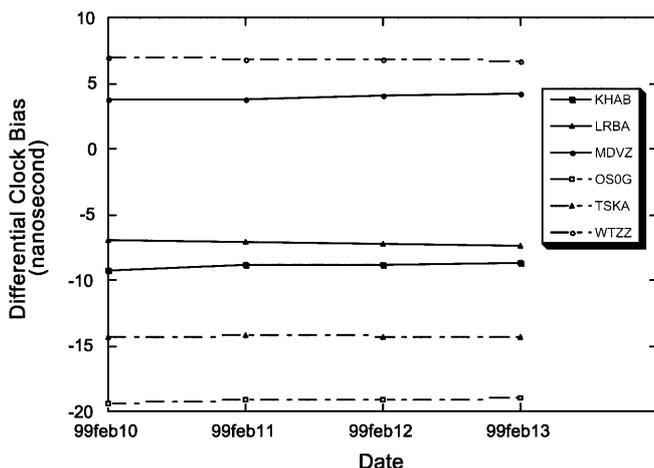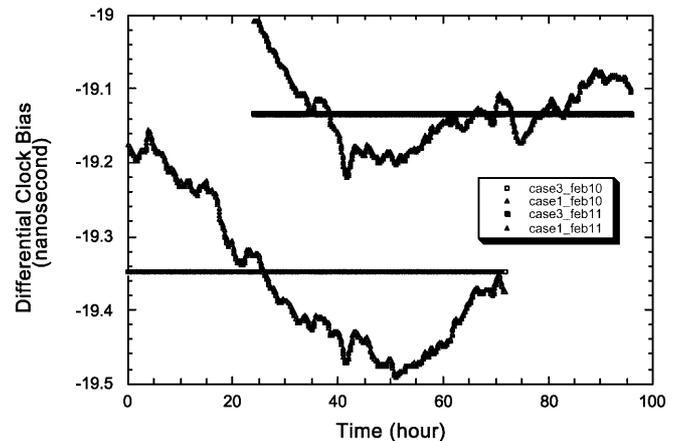

Fig. 6. Differential clock bias for site OS0G from two consecutive 3-day solutions
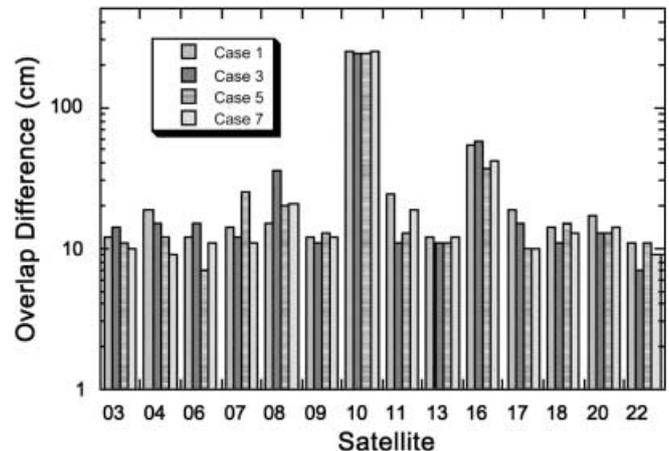

Fig. 7. Median orbit overlap difference for cases 1, 3, 5, and 7

quality of the GPS-based tropospheric delay parameters determined in the daily precise point positioning solution. The effect of the residual error of the tropospheric delay model on GLONASS orbit determination is, hence, negligible.

There are obvious residual tropospheric delay errors in cases 6 and 7. In those cases there are additional GLONASS tracking data with low elevation angle, while the GPS-based zenith tropospheric delay was determined using an elevation angle cut off at 15 degrees. Figure 3 shows that the data fit residual RMS in cases 6 and 7 are significantly higher than the ones in corresponding cases 1 and 3, respectively. However, the troposphere errors in those cases mostly stay in the data fit residual, the orbit overlap differences remains about the same or better compared with cases 1 and 3, as shown in Fig. 7. The orbit solutions appear to benefit from the improved data strength more than it suffers from the troposphere delay error.

In summary, using IGEX98 data we demonstrate GLONASS orbit determination accuracy at the 15-cm level, based on overlap differences. An independent evaluation of the orbit accuracy should follow with

Fig. 5. Differential clock biases for fiducial stations

available laser tracking data. Data strength is the most important factor that affects the orbit accuracy. Refining the solar radiation pressure force modeling for GLONASS satellites can effectively improve the orbit accuracy, especially for weak data. Temporal variations in the differential clock bias for dual-tracking receivers do not have a significant effect on the orbit determination at the present precision level. Similarly, the effect of inaccuracies in the daily GPS-based precise point positioning solutions is negligible.

References

Bertiger WI, Bar-Sever YE, Christensen EJ, Davis ES, Guinn JR, Haines BJ, Ibanez-Meier RW, Jee JR, Lichten SM, Melbourne WG, Muellerschoen RJ, Munson TN, Vigue Y, Wu SC, Yunck TP, Schutz BE, Abusali PAM, Rim HJ, Watkins MM, Willis P (1994) GPS precise tracking of TOPEX/POSEIDON: results and implications. J Geophys Res 99(C12): 24 449–24 469

Fliegel HF, Gallini TE, Swift ER (1992) Global positioning system radiation force model for geodetic applications. J Geophys Res 97(B1): 559–568

Haines BJ, Lichten SM, Srinivasan JM (1995) GPS-like tracking of geosynchronous satellites: orbit determination results for TDRS and INMARSAT. AAS/AIAA Astrodynamics Specialist Conference, paper AAS 95-372, Halifax, Nova Scotia, 14–17 August

Ineichen D, Rothacher M, Springer T, Beutler G (1999) Results of CODE as an analysis center of the IGEX-98 campaign. In: Slater JA et al (eds) Proc IGEX-98 Workshop, Nashville, TN, 13–14 September, pp 157–168

Jefferson DC, Bar-Sever YE, Heflin MB, Watkins MM, Webb FH, Zumberge JF (1999) JPL IGS Analysis Center Report, 1998. In: Gowey K et al (eds) International GPS Service for Geodynamics 1998 technical reports, pp 89–97, Jet Propulsion Laboratory, Pasadena

Kuang D, Bar-Sever Y, Bertiger WI, Hurst K, Zumberge J (1999) Determination of GLONASS satellite orbit at JPL — approach and results. Proc IGEX-98 workshop, Nashville, TN, 13–14 September, pp 201–208

Revnivykh S, Mitrikas V (1998) GEO-ZUP Company, GLONASS S/C mass and dimension, IGEX electronic mail message no. 0086, 23 November

Slater JA, Willis P, Gurtner W, Noll C, Beutler G, Hein G, Neilan RE (1998) The International GLONASS Experiment (IGEX-98). Proc ION GPS-98, Nashville, TN, 15–18 September

Wu SC (1985) Differential GPS approaches to orbit determination of high-altitude Earth satellites. In: Kaufman B et al (eds) Astrodynamics 1985, AAS/AIAA Astrodynamics Specialist Conference, paper AAS 85–430. Adv Astron Sci 58: 1203–1220, Univelt Inc., San Diego

Wu SC, Bar-Sever Y, Bassiri S, Bertiger WI, Hajj GA, Lichten SM, Malla RP, Trinkle BK, Wu JT (1990) Topex/Poseidon project: global positioning system (GPS) precision orbit determination (POD) software design. JPL D-7275, Jet Propulsion Laboratory, Pasadena

Ziebart M (1999) Analytical solar radiation pressure model for GLONASS: algorithm and initial results. Proc IGEX-98 Workshop, Nashville, TN, 13–14 September, pp 315–324

Zumberge JF, Heflin MB, Jefferson DC, Watkins MM, Webb FH (1997) Precise point positioning for the efficient and robust analysis of GPS data from large networks. J Geophys Res 102(B3): 5005–5017